Computers and Concrete, *Vol. 17, No. 1 (2016) 053-066*
DOI: http://dx.doi.org/10.12989/cac.2016.17.1.053

Chloride diffusion in concrete associated with single, dual and multi cation types

Zijian Song*, Linhua Jiang and Ziming Zhang

College of Mechanics and Materials, Hohai University, 1 Xikang road, Nanjing, China

(Received April 14, 2015, Revised December 24, 2015, Accepted January 7, 2016)

Abstract. Currently, most of the investigations on chloride diffusion were based on the experiments and simulations concerning single cation type chlorides. Chloride diffusion associated with dual or multi cation types was rarely studied. In this paper, several groups of diffusion experiments are conducted using chloride solutions containing single, dual and multi cation types. A multi-ionic model is also proposed to simulate the chloride diffusion behavior in the experimental tests. The MATLAB software is used to numerically solve the nonlinear PDEs in the multi-ionic model. The experimental and simulated results show that the chloride diffusion behavior associated with different cation types is significantly different. When the single cation type chlorides are adopted, it is found that the bound rates of chloride ions combined with divalent cations are greater than those combined with monovalent cations. When the dual/multi cation type chlorides are adopted, the chloride bound rates increase with the Ca^{2+}/Mg^{2+} percentage in the source solutions. This evidence indicates that the divalent cations would markedly enhance the chloride binding capacity and reduce the chloride diffusivity. Moreover, on the basis of the analysis, it is also found that the complicated cation types in source solutions are beneficial to reducing the chloride diffusivity.

Keywords: chloride diffusion; cation type; multi-ionic model; durability; concrete

1. Introduction

Chloride-induced reinforcement corrosion dominates the durability of reinforced concrete structures exposed to marine environments, salt lakes, de-icing salts etc (Yuan *et al*. 2009, Wang *et al*. 2012). A series of problems caused by chloride diffusion have drawn the attention of the worldwide researchers (Tang 1999, Paul *et al*. 2014, Tsao *et al*. 2015). In today's China, marine economy has become a national development strategy (Jiang *et al*. 2014, Zhao *et al*. 2014). A group of marine nuclear/wind power constructions would be built in the coming five years. In this situation, it becomes more necessary to study the diffusion behavior of chloride ions in concrete.

Diffusion behavior of chloride ions in concrete is generally affected by two important factors. One is concrete microstructure which contains pores, interface and cracks. The other is concrete chemical environment. The current researchers usually focused on the first factor. Nearly all their

---

*Corresponding author, Ph.D., E-mail: songzijian@hhu.edu.cn

http://www.techno-press.org/?journal=cac&subpage=8 ISSN: 1598-8198 (Print), 1598-818X (Online)

efforts were to enhance the concrete compactness and to improve the microstructure even though many of them perhaps were not really concerned with the micro-level. However, the factor of chemical environment was often selected to be ignored. The chemical environment means the ions, solid components and other chemicals surrounding the chloride ions, which would directly or indirectly influence the chloride diffusion behavior. The internal chemical environment is mainly referred to the major ions and the solid components existed in the cement-hydrated systems. The external chemical environment of chloride diffusion is mainly referred to the ions existed in the external environment.

It is very difficult to directly investigate the influence of the internal environment on chloride diffusion behavior since we can hardly change the internal chemical environment at the same time keep the concrete microstructure fixed. Fortunately, we can firstly study the influence of external chemical environment instead. As we know, chloride ions cannot diffuse solely without the company of cations or else the electro-neutrality would be broken up. K^+, Na^+, Ca^{2+} and Mg^{2+} are the common cation types existed in marine environments, salt lakes and de-icing salts (Jiang *et al*. 2012). The detailed cation compositions of different environments are quite different. Thus, it is necessary to study the diffusion behavior of chloride ions associated with these different cation types. Actually, many researchers have found the marked difference of the chloride diffusion behavior associated with different associated cation types (Zhu *et al*. 2012, Chatterji 1999, Arya *et al*. 1990). In the previous paper (Song *et al*. 2014), the authors also focused on this problem and built up a new model which could exactly predict the different diffusion behavior of chloride ions in concrete immersed in $CaCl_2$ and NaCl solutions. Unfortunately, those studies, including the authors` previous paper, were all on the basis of the experiments and simulations concerning single cation type chlorides. This is not in accordance with the real external environments.

In this paper, more diffusion experiments are conducted using chloride solutions containing single, dual and multi cation types. Meanwhile, a multi-ionic model is proposed to predict and analyze the chloride diffusion behavior. This paper is aimed to reveal the diffusion behavior of chloride ions associated with complicated cation types and meanwhile to validate the effectiveness of the multi-ionic model.

2. Experimental procedures

2.1 Materials and concrete mix

Type II Portland cement is used, the chemical compositions of which are given in Table 1. River sands with a fineness modulus of 2.8 and gravels with a maximum size of 20mm are utilized as the fine and coarse aggregates, respectively. The detailed concrete mix is given in Table 2.

Table 1 Composition of cement (wt. %)

Composition	SiO_2	Al_2O_3	Fe_2O_3	CaO	MgO	SO_3	Na_2O	K_2O	TiO_2	MnO_2	P_2O_5
Content	21.70	5.09	4.32	64.64	0.92	1.08	0.21	0.53	0.14	0.10	0.05

Table 2 Mixing proportions (kg/m^3)

w/c	cement	water	sand	gravel
0.50	312	156	746	1118

2.2 Specimens preparation

A concrete slab is prepared in size 2000 mm×1000 mm×20 mm. After casting, the slab is covered with a polythene sheet and stored in the laboratory air for 24 hours. Subsequently, the slab is demoulded and immediately put into saturated limewater for curing. The limewater tank is stored in a constant temperature-humidity room (20±1°C, 55±3% relative humidity) and also covered with a polythene sheet. After curing for 28 days, the slab is taken out and from which a group of cylinder specimens are drilled out. The cylinders are cut into $\Phi 100\times 50$ and then immediately put into saturated limewater for the continued curing.

2.3 Immersion test

After the required concrete age (90d) is reached, twenty-one groups of specimens are finally taken out for the following immersion test. The side and bottom surfaces of the cylinder specimens are sealed with epoxy resin while the top surface is exposed to the source solutions for 6 months. The solution tanks are covered with polythene sheets to avoid evaporations and carbonizations. Plus, the solutions are renewed every month for maintaining the chloride concentrations. The detailed source solutions used in this paper are listed in Table 3.

2.4 Powder sampling and chloride titration

After immersion, the concrete specimens are milled, layer by layer, into powder. The thickness of each layer is controlled within 1-3 mm. The powder from border area of each layer is discarded while the powder from core area is passed through a powerful magnet to remove the possible ferrous powder derived from the milling head. After that, the available powder is divided into two groups. One group is soaked in de-ionized water and the other one is soaked in dilute nitric acid solution to determine the water-soluble and total chloride concentration, respectively. The detailed procedures are similar to the methods introduced in the standard ASTM C1218/C1218M and ASTM C1152/C1152M, respectively. In the titration work, an automatic titrimeter is used to precisely determine the chloride concentrations.

Table 3 Source solutions used in immersion test

No.	Cation type	No.	Cation type	No.	Cation type
S1	0.5 M Na^+	S2	0.5 M K^+	S3	0.25 M Ca^{2+}
S4	0.25 M Mg^{2+}	M1	0.2 M Na^+ + 0.15 M K^++ 0.075 M Ca^{2+}	M2	0.2 M Na^+ + 0.15 M K^+ + 0.075 M Mg^{2+}
M3	0.2 M Na^+ + 0.075 M Mg^{2+}+ 0.075 M Ca^{2+}	M4	0.2MNa^+ + 0.1 M K^+ + 0.05 M Ca^{2+}+ 0.05 M Mg^{2+}	M5	0.43 M Na^+ + 0.01 M K^+ + 0.01 M Ca^{2+}+ 0.05MMg^{2+} +0.03M SO_4^{2-} (seawater)
D1	0.40 M Na^+ + 0.10 M K^+	D5	0.40 M Na^+ + 0.050 M Ca^{2+}	D9	0.40 M Na^+ + 0.050 M Mg^{2+}
D2	0.30 M Na^+ + 0.20 M K^+	D6	0.30 M Na^+ + 0.100 M Ca^{2+}	D10	0.30 M Na^+ + 0.100 M Mg^{2+}
D3	0.20 M Na^+ + 0.30 M K^+	D7	0.20 M Na^+ + 0.150 M Ca^{2+}	D11	0.20 M Na^+ + 0.150 M Mg^{2+}
D4	0.10 M Na^+ + 0.40 M K^+	D8	0.10 M Na^+ + 0.200 M Ca^{2+}	D12	0.10 M Na^+ + 0.200 M Mg^{2+}

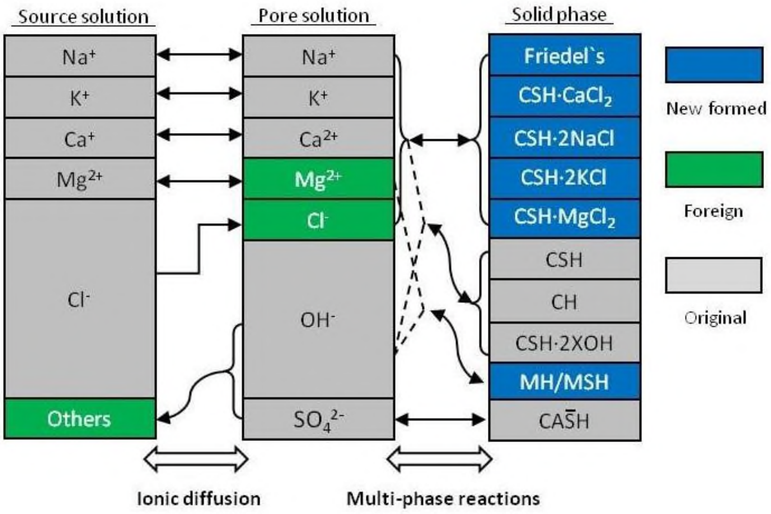

Fig. 1 Complicated physicochemical process of chloride diffusion

3. Numerical simulations

Chloride diffusion process in concrete is essentially a complicated physicochemical process that accompany with ionic actions and multi-phase reactions, as schematically shown in Fig. 1. The multi-species ionic diffusions between source and pore solutions would change the internal chemical environment and subsequently influence the chloride diffusion behavior in concrete. Thus, many conventional single-species ionic models, such as a series of Fick-based models, perhaps could not exactly represent the complicated diffusion process.

In the previous paper (Song *et al*. 2014), a model considering multi-phase reactions and ionic interactions was carried out to describe the chloride diffusion behavior in concrete. In this model, the governing equations of ions and solid components are considered as

$$\frac{\partial c_{i\pm}}{\partial t} = \frac{\partial}{\partial x}\left(D_{i\pm}\frac{\partial c_{i\pm}}{\partial x} \pm z_{i\pm}c_{i\pm}D_{i\pm}\frac{\sum z_{i-}D_{i-}\frac{\partial c_{i-}}{\partial x} - \sum z_{i+}D_{i+}\frac{\partial c_{i+}}{\partial x}}{\sum z_{i+}^{2}D_{i+}c_{i+} + \sum z_{i-}^{2}D_{i-}c_{i-}}\right) - r_{i\pm},\ \mathrm{i}=Na^{+},\ K^{+},\ Ca^{2+},\ Cl^{-},\ OH^{-},\ SO_{4}^{2-}. \tag{1}$$

$$\frac{\partial c_{sol}}{\partial t} = r_{sol},\ sol = CH,\ CSH,\ CSH\cdot CaCl_{2},\ CSH\cdot 2NaCl,\ CSH\cdot 2KCl,\ CSH\cdot 2NaOH,\ CSH\cdot 2KOH,\ CAH,\ CASH,\ Friedel`s\ salt. \tag{2}$$

Where, c_{i+} and c_{i-} are the concentrations of the positively and negatively charged ions, j_{i+} and j_{i-} are the ionic flux of the positively and negatively charged ions respectively, r_{i+} and r_{i-} are the mass change of the positively and negatively charged ions caused by multiphase reactions, D_{i+} and D_{i-} are the diffusion coefficients associated with these ions, z_{i+} and z_{i-} are the associated ionic valences, *c*sol is the concentrations of the solid phases, *r*sol is the mass change of the solid phases caused by multiphase reactions. Moreover, the diffusion coefficients of the ions in concrete are equal to

$$D_{i\pm} = D_s \tau D_{i\pm}^0 \tag{3}$$

Where, D_{i+}^0 and D_{i-}^0 are the diffusion coefficients of the positively and negatively charged ions in bulk water, τ is the correlation factor associated with the pore geometry of concrete, D_s is a correction factor associated with the effect of double electrical layers.

The rates of the multiphase reactions are listed as below

$$r_1 = s_{CH}\left(k_d^{CH} - k_a^{CH}\left(\left[Ca^{2+}\right]\left[OH^-\right]^2\right)^{n_1}\right) \tag{4}$$

$$r_2 = k_d^{CSH}[C/S] - k_a^{CSH}\left([Ca^{2+}][OH^-]^2\right)^{n_2} \tag{5}$$

$$r_3 = k_a^{CSH\cdot CaCl_2}[CSH\cdot CaCl_2] - k_d^{CSH\cdot CaCl_2}\left([Ca^{2+}][Cl^-]^2\right)^{n_3} \tag{6}$$

$$r_4 = k_a^{CSH\cdot CaCl_2}[CSH\cdot 2NaCl] - k_d^{CSH\cdot CaCl_2}\left([Na^+]^2[OH^-]^2\right)^{n_4} \tag{7}$$

$$r_5 = k_a^{CSH\cdot 2KCl}[CSH\cdot 2KCl] - k_d^{CSH\cdot 2KCl}\left([K^+]^2[OH^-]^2\right)^{n_5} \tag{8}$$

$$r_6 = k_a^{CSH\cdot 2NaOH}[CSH\cdot 2NaOH] - k_d^{CSH\cdot 2NaOH}\left([Na^+]^2[OH^-]^2\right)^{n_6} \tag{9}$$

$$r_7 = k_a^{CSH\cdot 2KOH}[CSH\cdot 2KOH] - k_d^{CSH\cdot 2KOH}\left([K^+]^2[OH^-]^2\right)^{n_7} \tag{10}$$

$$r_8 = k_a^{CAH}[CAH] - k_d^{CAH}\left([Ca^{2+}][OH^-]^2\right)^{n_8} \tag{11}$$

$$r_9 = k_d^{CA\bar{S}H}[CA\bar{S}H]^{\alpha} - k_a^{CA\bar{S}H}\left([Ca^{2+}][SO_4^{2-}]\right)^{n_9} \tag{12}$$

$$r_{10} = k_d^{CAHCaCl_2}[CAHCaCl_2] - k_a^{CAHCaCl_2}\left([Ca^{2+}][Cl^-]^2\right)^{n_{10}} \tag{13}$$

Where, the parameter k_d^x is used to represent the dissolution or desorption rate constant of the component *X* while k_a^x is used to represent the absorption or formation rate constant of *X*. The parameters ri and *n*i (i= 1, 2, 3…10) are used to represent the reaction rate and the reaction order of the associated reaction.

In this paper, the equations associated with Mg^{2+} are newly added into this model since Mg^{2+} is employed in the source solutions. Brucite is considered to be the main production in the presence of Mg^{2+} in the pore solution with concentrated OH-. Considering the formation of Brucite is fast and almost irreversible, the reaction rate is described as

$$r_{11} = -k_a^{\mathrm{MH}}\left(\left[Mg^{2+}\right]\left[OH^-\right]^2\right)^{n_{11}} \tag{14}$$

The Mg^{2+} ions are also considered to be physically bound in the C-S-H with the chloride, especially in the absence of the hydroxyl. The binding rate is described as

$$r_{12} = k_d^{CSH\cdot MgCl_2}[CSH\cdot MgCl_2] - k_a^{CSH\cdot MgCl_2}\left([Mg^{2+}][Cl^-]^2\right)^{n_3} \tag{15}$$

Based on the reaction rates, the mass changes of the ions and the solid components mentioned in Eqs. (1)-(2) are obtained and listed as below

Solid phase: $r_{CH} = -r_1$, $r_{CSH} = -r_2$, $r_{C/S} = -r_2/8.84$, $r_{CSH2NaCl} = -r_3$, $r_{CSH2NaCl} = -r_4$, $r_{CSH2KCl} = -r_5$, $r_{CSH2NaOH} = -r_6$, $r_{CSH2KOH} = -r_7$, $r_{CAH} = -r_8$, $r_{CA\bar{S}H} = -r_9$, $r_{Frediel} = -r_{10}$, $r_{\mathrm{MH}} = -r_{11}$, $r_{CSHMgCl_2} = -r_{12}$

Ions: $r_{Na^+} = 2r_4 + 2r_6$, $r_{K^+} = 2r_5 + 2r_7$, $r_{Ca^{2+}} = r_1 + r_2 + r_3 + r_8 + r_9 + r_{10}$, $r_{SO_4^{2-}} = r_9$, $r_{Cl^-} = 2r_3 + 2r_4 + 2r_5 + 2r_{10} + 2r_{11}$, $r_{Mg^{2+}} = r_{11} + r_{12}$

A simple trial and error method (Johannesson *et al.* 2007) is applied to fix the rate constants of the multi-phase reactions. The MATLAB software (the pdepe function) is used to numerically solve the nonlinear PDEs in the mathematical model. Since the multi-ionic model takes into account the ionic interactions and the major multiphase reactions in concrete, this model is considered to be applicable to predict the chloride diffusion behavior in more complicated chemical environments. The purpose of the simulation in this investigation is mainly to analyze the diffusion behavior of chloride ions associated with different cation types, and by the way to demonstrate the effectiveness of the multi-ionic model.

4. Results and discussion

4.1 Chloride profiles

Fig. 2 typically shows several groups of measured and simulated concentration profiles of total chloride ions in concrete immersed in chloride solutions associated with different cation types. For each simulated curve, the data of three concrete specimens (the scatter points in the same color) were given in comparison. Ignoring the ineviTable experimental errors, it can be safely concluded that the test results and the simulation results generally fit well with each other, which demonstrate the effectiveness of the multi-ionic model.

The chloride concentration profiles associated with different cation types are very different. By comparing the results of the test groups associated with single cation types, it is found that the concentrations of Cl^- combined with divalent cations are much greater than those combined with monovalent cations and the detailed order is $CaCl_2 > MgCl_2 > NaCl \approx KCl$. This trend is the same as Goto's results (Goto and Roy 1981). The results of chloride concentrations associated with dual cation types generally fall in between the results associated with the two relative single cation types, and meanwhile they are a little larger than the weighted mean values associated with the two single cation types. For example, as shown in Fig. 2(a), c_{Cl^-}(0.5M NaCl)<c_{Cl^-}(0.1M $CaCl_2$+0.3M NaCl)<c_{Cl^-}(0.25M $CaCl_2$), and c_{Cl^-}(0.1M $CaCl_2$+0.3MNaCl)>60%c_{Cl^-}(0.5M NaCl)+40%c_{Cl^-}(0.25M

$CaCl_2$). The results of multi cation types get similar rules. For example, as shown in Fig. 2(d), c_{Cl-}(0.2M NaCl+0.3M KCl)<c_{Cl-}(0.2M NaCl+0.15M KCl+0.075M CaCl2)<c_{Cl-}(0.2M NaCl+0.15M $CaCl_2$).

It is also noticed that the total chloride concentration profiles of NaCl, KCl, $MgCl_2$ and their composite solutions have a concentration drop near the specimen surface. This kind of chloride drops were frequently found in the unsaturated concrete undergoing water dry/wet alternation (Sleiman *et al*. 2012, Arya *et al*. 2014). However, in this investigation, the unexpected chloride drop is perhaps due to the fact that the Ca^{2+} ions in the pore solution of concrete immersed in these solutions would be leached out and the binding rate would be getting slower in the absence of Ca^{2+} ions. Thus, with the increase of Ca^{2+} concentration in the source solutions, the chloride drop near

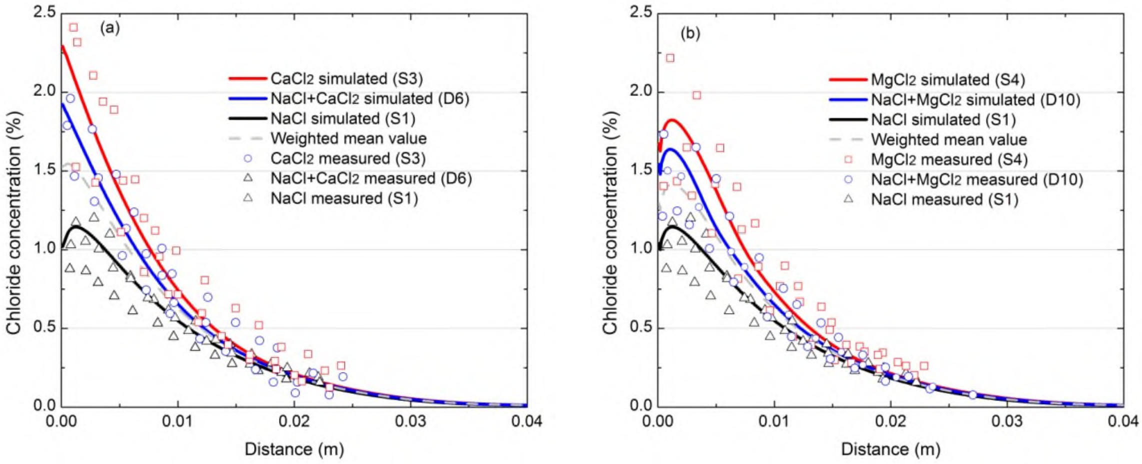

(a) NaCl, NaCl+$CaCl_2$, $CaCl_2$ (b) NaCl, NaCl+$MgCl_2$, $MgCl_2$

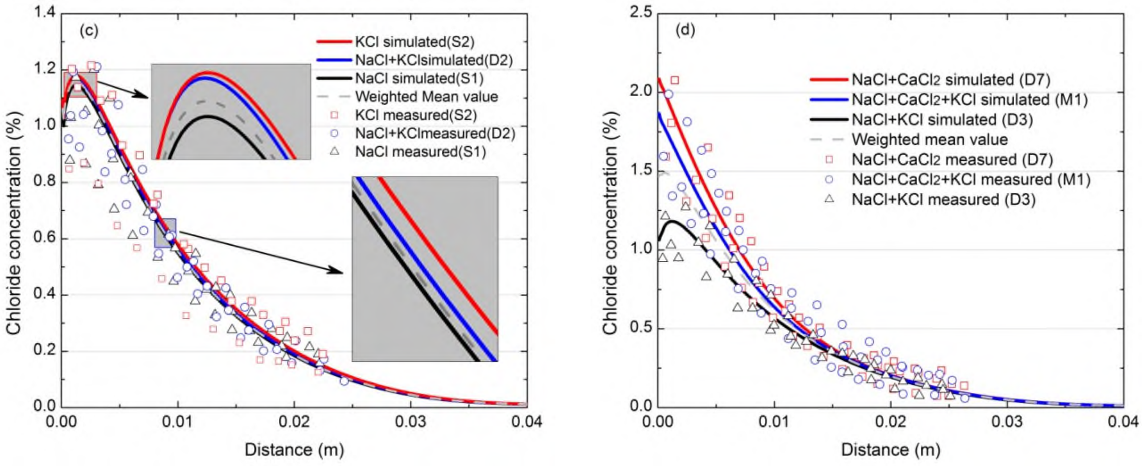

(c) NaCl, NaCl+KCl, KCl (d) NaCl+$CaCl_2$, NaCl+$CaCl_2$+KCl, NaCl+KCl

Fig. 2 Measured and simulated concentration profiles of total chloride ions in concrete specimens immersed in different chloride solutions

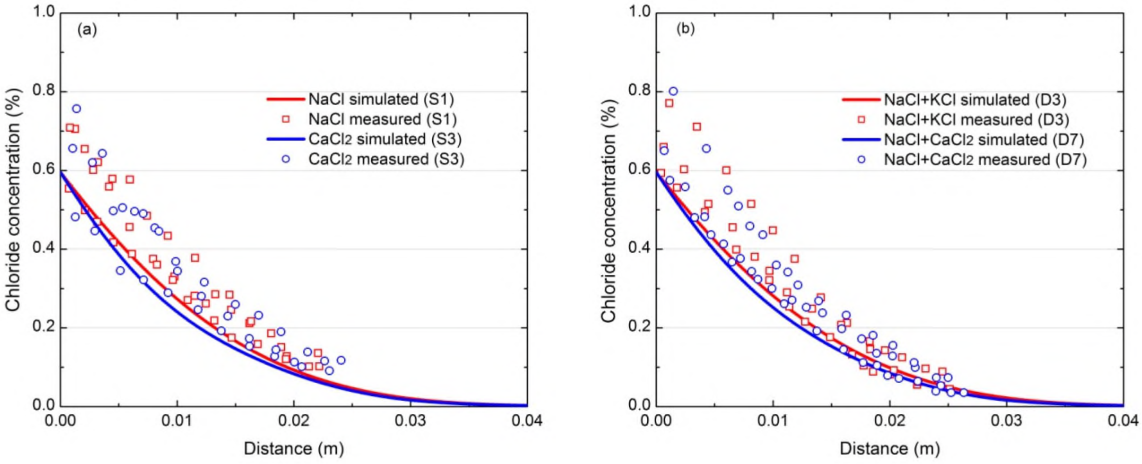

(a) NaCl, $CaCl_2$ (b) NaCl+KCl, NaCl+$CaCl_2$

Fig. 3 Measured and simulated concentration profiles of free chloride ions in concrete specimens immersed in different chloride solutions

the surface gradually disappears.

Fig. 3 typically shows the free (water-soluble) chloride concentration profiles of concrete specimens immersed in different solutions. Comparing with total chloride concentration profiles, the free chloride concentration profiles associated with different cation types are not so much different. In addition, the unexpected chloride drops existed in total profiles neither present at the free chloride concentration profiles. This indicates that the major differences in total chloride profiles were derived from the chloride bound capacity. It’s also found that the free chloride concentrations are a little bigger than predicted. This is possibly because the determining method of water-soluble chloride would break the balance of chloride binding and release out of more free chloride ions. Actually, many researchers also found that the water-soluble method would over-estimate the free concentrations (Otsuki *et al*. 1993, He *et al*. 2009, Haque and Kayyali 1995). The similar results of those researchers indirectly prove the rationality of the present model.

4.2 Chloride binding capacity

Fig. 4 shows the measured and simulated relationships between bound chloride concentrations and free chloride concentrations. It’s noticed that the binding rule in the unsteady diffusion test is different from the Freundlich or the Langmuir binding isotherm which was frequently obtained in laboratory (Delagrave *et al*. 1997, Glass and Buenfeld 2000, Mien *et al*. 2014, Zibara 2001). Oppositely, the measured relationships are more similar to the linear rule obtained in the field engineering and other unsteady situations (Sandberg 1999, Mohanmmed and Hamada 2003, Mangat and Molloy 1995, Amiri *et al*. 2006). Actually, we can easily found in the simulated results that the rules are not really linear. The slopes of the simulated curves vary with the range of the distance, so the bound rates also vary with the range of distance. The max or min bound rate is neither found in the surface nor in the deepest, which is different from all the existed binding isotherms. This indicates that the bound rates are perhaps not a simple function of free chloride concentrations but influenced by many factors, such as cation type and ‘chloride-binding time’.

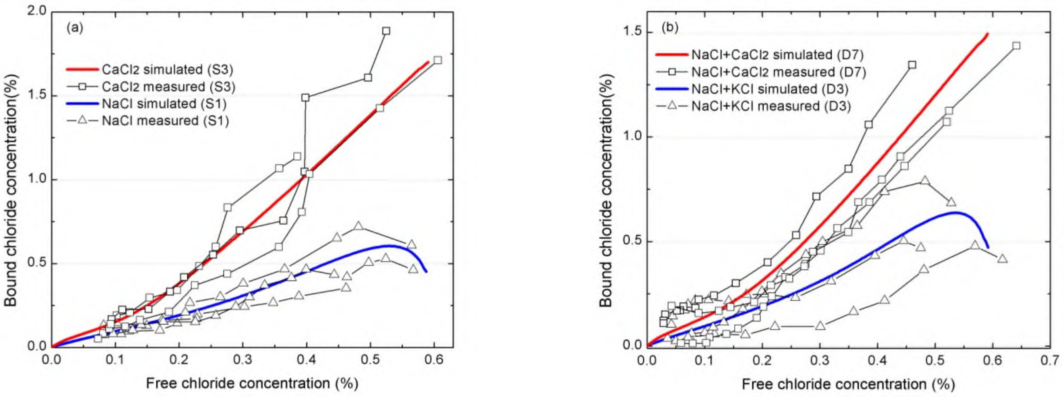

(a) NaCl, $CaCl_2$ (b) NaCl+KCl, NaCl+$CaCl_2$

Fig. 4 Measured and simulated relationships between bound and water-soluble chloride concentrations

Here the ‘chloride-binding time’ is defined as the duration from the chloride ions first contact the solid phase until the test ends. Obviously, the cation types and chloride-binding times in different distances are mostly different. Thus, it explains why the bound rates vary with the distance.

The water-soluble concentrations ($c_{w.s}$) were frequently used to substitute the free chloride concentrations (c_f) in the calculations of chloride bound rates. However, many researchers found that the free chloride concentrations are a little bigger than the water-soluble concentrations. If the linear relationship *cw.s=kcf* is assumed (He *et al*. 2009), the chloride bound rates can be corrected using Eq. (15).

$$\beta_f = \frac{\beta_w + k - 1}{k} \tag{16}$$

Where, β_f is the chloride bound rates calculated from the free chloride concentrations, β_w is the chloride bound rates calculated from the water soluble chloride concentrations. In this research, the k is approximately equal to 1.25 which is obtained by a simple linear fitting. According to this, the bound rates were corrected and shown in Table 4. It can be found in Table 4 that the surface bound rates of chloride ions associated with different cation types vary in a range from 40% to 80%. Considering the results associated with single cation types, it is found that the bound rates of chloride ions with divalent cations are greater than those combined with monovalent cations and they decrease in the order of $Ca^{2+}>Mg^{2+}>Na^{+}\approx K^{+}$. This trend is similar to the previous workers` results (Zhu *et al*. 2012, Arya *et al*. 1990). The chloride bound rates associated with dual cation types generally fall in between the results associated with the two relative single cation types, and meanwhile they are a little larger than the weighted mean values of the two single cation types. The rules of multi-cation types are similar. This phenomenon indicates that the complicated cation types in source solutions would benefit the chloride binding. Plus, it is also noticed that the chloride bound rates increase with the averaged cation valence of the source solutions. This evidence further proves that the divalent cations would markedly enhance the binding capacity of chloride ions.

Table 5 Chloride bound rates calculated from measured results and simulated results

No.	Bound rate			No.	Bound rate			No.	Bound rate		
	surface	max	min		surface	max	min		surface	max	min
S1	48.79 (42.60)	58.60 (53.92)	40.43 (40.80)	S2	49.35 (45.42)	56.28 (54.59)	44.45 (42.40)	S3	75.60 (79.35)	75.96 (79.35)	51.21 (52.75)
S4	70.86 (64.40)	74.08 (72.55)	58.06 (52.82)	M1	75.46 (73.79)	72.68 (73.79)	46.25 (50.33)	M2	65.64 (61.15)	67.37 (65.98)	51.81 (50.22)
M3	81.56 (77.02)	76.85 (77.02)	52.09 (51.67)	M4	75.37 (75.21)	78.67 (75.21)	53.79 (50.74)	M5	70.05 (68.18)	72.16 (68.18)	51.13 (49.91)
D1	48.89 (44.63)	58.96 (54.41)	40.16 (42.10)	D5	67.75 (70.92)	68.07 (70.92)	45.88 (50.05)	D9	62.89 (58.39)	64.67 (63.17)	48.27 (49.93)
D2	49.54 (45.47)	57.61 (54.69)	46.63 (42.65)	D6	72.98 (74.90)	76.91 (74.90)	48.55 (51.04)	D10	68.02 (61.36)	65.14 (67.44)	55.76 (50.97)
D3	48.82 (45.94)	63.95 (54.83)	36.24 (42.92)	D7	70.32 (77.03)	77.35 (77.03)	44.05 (51.75)	D11	66.97 (62.99)	70.21 (69.82)	51.16 (51.73)
D4	49.43 (46.07)	60.45 (54.83)	39.32 (42.95)	D8	77.58 (78.42)	76.23 (78.42)	53.69 (52.30)	D12	70.62 (63.99)	74.99 (71.41)	57.14 (52.33)

*The data in round brackets are calculated from simulated results.

4.3 Apparent diffusion coefficients and apparent surface concentrations

Fick's 2nd law is used to fit the total chloride conentrations. Two important parameters are obtained in the fitting curves. One is the apparent diffusion coefficient. The other is the apparent surface concentration. If considering group S1 (0.5mol/L NaCl) as the control group, and meanwhile defining the apparent diffusion coefficent and apparent surface concentration of this group as the standard values, then the two parameters of other groups are equal to the standard values multipy the correction factors, namely c_s (Cl- with other cations) =$\beta_1 . c_s$ (NaCl), D_{app}(Cl- with other cations) =$\beta_2 \cdot D_{\text{app}}$(NaCl).

Based on the definition, the correction factors β_1 and β_2 of the different source solutions are solved out and shown in Table 5. It is found in Table 5 that β_1 and β_2 change obviously with the combined cation types. From the β_2 values of the test groups associated with single cation types (groups S1-S4), it is found that the apparent diffusion coefficients of chloride ions combined with divalent cations are smaller than those combined with monovalent cations and they increase in the order of $Ca^{2+}<Mg^{2+}<Na^{+}\approx K^{+}$. From the β_1 values of the test groups associated with single cation types, it is found that the trend of the apparent surface concentrations is just opposite to the trend of apparent diffusion coefficients. In fact, the same trend has appeared in the previous researchers` investigations (Goto *et al.* 1981, Zhang and Gjørv 1994) though the correct analysis was not given in those investigations. Fig. 5 shows the variations trends of β_1 and β_2 in the conditions of dual cation types. It is found that, when dual cation types are adopted, Ca^{2+} and Mg^{2+} have marked influence on the chloride diffusion coeffcients. The chloride diffusion coefficients decline considerably with the increase of the Ca^{2+}/Mg^{2+} percentage. By comparison, the influence of K+ is relatively small. Nevetheless, with the increase of the K^{+} percentage, the chloride diffusion coefficients still have a negilibly growth. It is noticed that the divalent cations also have a marked influence on the apparent surface conentrations. The apparent surface conentrations increase markedly with the Ca^{2+}/Mg^{2+} percentage. The influence of K^{+} is also very small. With the increase of the K^{+} percentage, the chloride diffusion coefficients have a negilibly growth.

Table 6 Correction factors β_1 and β_2 calculated from measured results and simulated results

No.	Correction factor		No.	Correction factor		No.	Correction factor	
	β_1	β_2		β_1	β_2		β_1	β_2
S1	1.000 (1.000)	1.000 (1.000)	S2	1.029 (1.030)	1.018 (1.051)	S3	1.962 (1.770)	0.671 (0.651)
S4	1.685 (1.620)	0.798 (0.775)	M1	1.483 (1.422)	0.810 (0.736)	M2	1.461 (1.382)	0.817 (0.820)
M3	1.705 (1.657)	0.681 (0.676)	M4	1.452 (1.550)	0.692 (0.710)	M5	1.413 (1.331)	0.850 (0.805)
D1	1.063 (1.014)	1.012 (0.997)	D5	1.213 (1.311)	0.761 (0.769)	D9	1.281 (1.252)	0.871 (0.867)
D2	1.035 (1.023)	0.972 (1.000)	D6	1.591 (1.485)	0.695 (0.711)	D10	1.421 (1.405)	0.788 (0.809)
D3	1.053 (1.029)	1.031 (1.013)	D7	1.642 (1.606)	0.666 (0.682)	D11	1.473 (1.504)	0.795 (0.787)
D4	1.097 (1.031)	1.019 (1.028)	D8	1.714 (1.698)	0.651 (0.663)	D12	1.615 (1.573)	0.771 (0.778)

*The data in round brackets are calculated from simulated results.

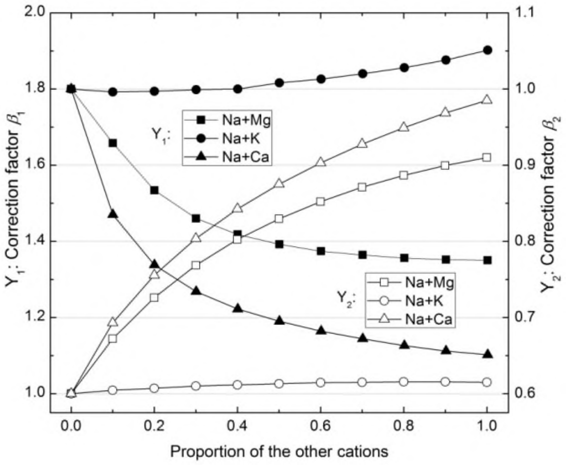

Fig. 5 Change trends of correction factors in source solutions with dual cation type

It is noticed that, all the curves of β_1 in Fig. 5 are concave functional. Meanwhile, all the curves of β_2 in Fig. 5 are convex functional. In other words, for any source solutions containing dual cation types, the apparent chloride diffusion coefficients and the apparent surface chloride concentrations would comply with the following equations

$$c_s\left(Cl^- \ of \ w_1A+w_2B\right) > w_1c_s\left(Cl^- \ of \ A\right)+w_2c_s\left(Cl^- \ of \ B\right) \tag{17}$$

$$D_{app}\left(Cl^- \ of \ w_1A+w_2B\right) < w_1D_{app}\left(Cl^- \ of \ A\right)+w_2D_{app}\left(Cl^- \ of \ B\right) \tag{18}$$

Where, w_1 is percentage of chloride ions possessed by cation A; w_2 is percentage of chloride ions possessed by cation B. Plus, it also can be seen from Table 6 that the diffusion behavior of chloride ions combined with multi cation types have similar regulations, for example: D_{app}(Cl^- of 0.2M Na^++0.075M Mg^{2+}+0.075M Ca^{2+})=0.676<0.828=40%×D_{app}(Cl^- of 0.5M Na^+)+30%× D_{app}(Cl^- of 0.25M Mg^{2+})+30%×D_{app}(Cl^- of 0.25M Ca^{2+}); c_s(Cl^- of 0.2M Na^++0.075M Mg^{2+}+0.075M Ca^{2+})=1.657<1.417=40%×c_s(Cl^- of 0.5M Na^+)+30%×c_s(Cl^- of 0.25M Mg^{2+})+ 30%×c^s(Cl^- of 0.25M Ca^{2+}). This rule indicates that the complicated cation types in source solutions are beneficial to reducing the chloride diffusivity.

5. Conclusions

Based on the discussion above, the following conclusions can be drawn:

- The multi-ionic model is confirmed to be effective to predict the diffusion behavior of chloride ions associated with complicated cation types.
- The total chloride concentration profiles associated with different cation types are very different while the free ones are not so much different. This indicates that the major differences in total chloride profiles are derived from the chloride bound capacity.
- The total chloride concentration profiles of the source solutions containing Na^+, K^+ or Mg^{2+} have a concentration drop near the concrete surface. However, the chloride drop near the surface gradually disappears along with the increase of Ca^{2+} in the source solutions.
- The binding rules in the unsteady diffusion test are different from the Freundlich or the Langmuir binding isotherms obtained in laboratory. Oppositely, the relationships are more similar to be the linear rule obtained in the field engineering.
- Considering the results of the test groups associated with single cation types, the bound rates of chloride ions combined with divalent cations are greater than those combined with monovalent cations and they decrease in the order of $Ca^{2+}>Mg^{2+}>Na^{+}\approx K^{+}$. For the results associated with dual and multi cation types, the chloride bound rates increase with the averaged cation valence of the source solutions. This evidence further proves that the divalent cations would markedly enhance the binding capacity of chloride ions.
- The bound rates of chloride ions with dual cation types generally fall in between the results associated with the two relative single cation types, and meanwhile they are a little larger than the weighted mean values of the results associated with the two single cation types.
- Considering the results associated with single cation types, the apparent diffusion coefficients of chloride ions combined with divalent cations are smaller than those combined with monovalent cations and they decrease in the order of $Ca^{2+}<Mg^{2+}<Na^{+}\approx K^{+}$. For the results associated with dual and multi cation types, the apparent diffusion coefficients increase markedly with the Ca^{2+}/Mg^{2+} percentage in the source solutions.
- For the source solutions containing dual cations, the apparent chloride diffusion coefficients are smaller than the weighted mean values of the results associated with the two single cation types. Meanwhile, the apparent surface chloride concentrations are larger than the weighted mean values. The detailed relationships are shown in Eqs. (16)-(17).

Acknowledgments

The authors wish to acknowledge the financial support by the National Natural Science

Foundation of China under Project Nos. 51278167 and 51479051. The supports of State Key Laboratory of Hydrology-Water Resources and Hydraulic Engineering are also appreciated.

References

Amiri, O., Friedmann, H. and Aït-Mokhtar, A. (2006), “Modelling of chloride-binding isotherm by multi-species approach in cement mortars submitted to migration test”, *Mag. Concrete Res.*, **58**(2), 93-99.

Arya, C., Buenfeld, N.R. and Newman, J.B. (1990), “Factors influencing chloride binding in concrete”, *Cement Concrete Res.*, **20**(2), 291-300.

Arya, C., Vassie, P. and Bioubakhsh, S. (2014), “Modelling chloride penetration in concrete subjected to cyclic wetting and drying”, *Mag. Concrete Res.*, **66**(7), 364-376.

Chatterji, S. (1999), “Transportation of ions through cement based materials: Part 3 Experimental evidence for the basic equations and some important deductions”, *Cement Concrete Res.*, **24**(7), 1229-1236.

Delagrave, A., Marchand, J., Olliver, J.P., Julien, S. and Hazrati, K. (1997), “Chloride binding capacity of various hydrated cement systems”, *Adv. Cement Based Mater.*, **6**(1), 28-35.

Glass, G.K. and Buenfeld, N.R. (2000), “The influence of chloride binding on the chloride induced corrosion risk in reinforced concrete”, *Corrosion Sci.*, **42**(2), 329-344.

Goto, S. and Roy, D.M. (1981), “Diffusion of ions through hardened cement pastes”, *Cement Concrete Res.*, **11**(5), 751-757.

Haque, M.N. and Kayyali, O.A. (1995), “Free and water soluble chloride in concrete”, *Cement Concrete Res.*, **25**(3), 531-542.

He, F.Q., Shi, C.Q., Yuan Q. and Zheng, K.R. (2009), “AgNO3 colorimetric method used for measuring chloride migration in concrete”, *J. Chin. Ceram. Soc.*, **37**(7), 1229-1234. (in Chinese)

Jiang, L.H., Huang, G.H., Xu, J.X, Zhu, Y.R. and Mo, L.L. (2012), “Influence of chloride salt type on threshold level of reinforcement corrosion in simulated concrete pore solutions”, *Constr. Build. Mater.*, **30** (1), 516-521.

Jiang, X.Z., Liu, T.Y. and Su, C.W. (2014), “China’s marine economy and regional development”, *Mar. Policy*, **50**, 227-237.

Johannesson, B., Yamada, K., Nilsson, L.O. and Hosokawa, Y. (2007), “Multi-species ionic diffusion in concrete with account to interaction between ions in the pore solution and the cement hydrates”, *Mater. Struct.*, **40**(7), 651-665.

Mangat, P.S. and Molloy, B.T. (1995), “Chloride binding in concrete containing PFA, gbs or silica fume under sea water exposure”, *Mag. Concrete Res.*, **47**(171), 129-141.

Mien, V.T., NAWA, T. and Stitmannaithum, B. (2014), “Chloride binding isotherms of various cements basing on binding capacity of hydrates”, *Comput. Concrete*, **13**(6), 695-707.

Mohanmmed, T.U. and Hamada, H. (2003), “Relationship between free chloride and total chloride contents in concrete”, *Cement Concrete Res.*, **33**(9), 1487-1490.

Otsuki, N., Nagataki, S. and Nakashita, K. (1993), “Evaluation of $AgNO_3$ solution spray method for measurement of chloride penetration into hardened cementitious matrix materials”, *Constr. Build. Mater.*, **7**(4), 195-201.

Paul, S.K., Chaudhuri, S. and Barai, S.V. (2014), “Chloride diffusion study in different types of concrete using finite element method (FEM)”, *Adv. Concrete Constr.*, **2**(1), 39-56.

Tsao, W.H., Huang, N.M. and Liang, M.T. (2015), “Modelling of chloride diffusion in saturated concrete”, *Comput. Concrete*, **15**(1), 127-140.

Sandberg, P. (1999), “Studies of chloride binding in concrete exposed in a marine environment”, *Cement Concrete Res.*, **29**(4), 473-477.

Sleiman, H., Amiri, O., Ait-Mokhtar, A. and Loche, J. (2012), “Chloride transport through unsaturated concrete: chloride profile simulations and experimental validation”, *Mag. Concrete Res.*, **64**(4), 351-359.

Song, Z.J., Jiang, L.H., Chu, H.Q. Xiong, C.X., Liu, R. and You, L.X. (2014), “Modelling of chloride diffusion in concrete immersed in $CaCl_2$ and NaC_l solutions with account of multi-phase reactions and ionic interactions", *Constr. Build. Mater.*, **66**(1), 1-9.

Tang, L.P. (1999), "Concentration dependence of diffusion and migration of chloride ions Part 1. Theoretical considerations", *Cement Concrete Res.*, **29**(9), 1463-1468.

Wang, X.Y., Park, K.B. and Lee, H.S. (2012), "Modeling of chloride diffusion in a hydrating concrete incorporating silica fume", *Comput. Concrete*, **10**(5), 523-539.

Yuan, Q., Shi, C.J., Schutter, G.D., Audenaert, K. and Deng, D.H. (2009), "Chloride binding of cement-based materials subjected to external chloride environment - A review", *Constr. Build. Mater.*, **23**(1), 1-13.

Zhang, T.W. and Gjørv, O.E. (1994), "An electrochemical method for accelerated testing of chloride diffusivity in concrete", *Cement Concrete Res.*, **24**(8), 1534-1548.

Zhao, R., Hynes, S. and He, G.S. (2014), "Defining and quantifying China's ocean economy", *Mar. Policy*, **43,** 164-173.

Zhu, Q., Jiang, L.H., Chen, Y., Xu, J.X. and Mo, L.L. (2012), "Effect of chloride salt type on chloride binding behavior of concrete", *Constr. Build. Mater.*, **37**(1), 512-517.

Zibara, H. (2001), "Binding of external chloride by cement pastes", Ph.D. Dissertation, University of Toronto, Toronto, Canada.

CC